

**Paper 6-1** has been designated as a Distinguished Paper at Display Week 2018. The full-length version of this paper appears in a Special Section of the *Journal of the Society for Information Display (JSID)* devoted to Display Week 2018 Distinguished Papers. This Special Section will be freely accessible until December 31, 2018 via:

[http://onlinelibrary.wiley.com/page/journal/19383657/homepage/display\\_week\\_2018.htm](http://onlinelibrary.wiley.com/page/journal/19383657/homepage/display_week_2018.htm)

Authors that wish to refer to this work are advised to cite the full-length version by referring to its DOI:

<https://doi.org/10.1002/jsid.654>

# Design Strategies for Materials Showing Thermally Activated Delayed Fluorescence and Beyond: Towards the Fourth-generation OLED Mechanism

Hartmut Yersin\*, Larisa Mataranga-Popa, Shu-Wei Li, Rafal Czerwieniec

Institute for Physical Chemistry, University of Regensburg, 93040 Regensburg, Germany  
hartmut.yersin@ur.de

## Abstract

Design strategies for TADF molecules are discussed and a new emitter concept based on an almost “zero-energy-gap” is developed. Thermal activation is not substantial. Applied in an OLED, all singlet and triplet excitons are harvested directly in the lowest singlet state without time-delaying TADF. This landmarking mechanism, being beyond TADF, leads to emission decay times in the sub- $\mu$ s range.

## Keywords

Direct Singlet Harvesting, DSH mechanism, thermally activated delayed fluorescence, TADF, OLED mechanism beyond TADF, new organic emitter materials, short decay time

## 1. Introduction

More than one decade ago, use of thermally activated delayed fluorescence (TADF) [1] has been proposed as harvesting mechanism for singlet and triplet excitons that are generated in the emission layer of an OLED. [2] Meanwhile, the development of this new technology is characterized by an exceptional interdisciplinary research in the fields of chemistry, physics, and material sciences. [3] To obtain attractive TADF materials, it has to be focused especially on short TADF decay times (at high photoluminescence quantum yields) to avoid saturation effects and to reduce stability problems, which frequently occur when populating excited states. For many TADF materials, one can observe relatively short TADF decay times lying in the range of several  $\mu$ s. [4] However, mostly additional long tails with decay times in the ms range are also occurring. As a consequence, successful TADF materials should exhibit a series of structure/property motifs: (i) The compounds should show small energy separations  $\Delta E(S_1-T_1)$  between the lowest singlet  $S_1$  and triplet  $T_1$  state. This can be achieved by developing molecular structures with spatially largely separated HOMO and LUMO, which provides small exchange interaction and thus, small  $\Delta E(S_1-T_1)$ . (ii) On the other hand, at least weak HOMO-LUMO overlap should still be maintained to guarantee a residual allowedness of the fluorescence transition.[5] (iii) The exchange interaction or the HOMO-LUMO overlap should be homogeneous over the ensemble of the TADF molecules. Otherwise, distinct inhomogeneity effects would result that induce variations of  $\Delta E(S_1-T_1)$  and thus, for example, long TADF decay tails. (iv) Fast TADF decay requires fast down-intersystem crossing (down-ISC) and fast up-ISC. However, for purely organic compounds, this is not always realized even for small  $\Delta E(S_1-T_1)$  gaps, since pure singlet and triplet states that result from the same configuration do not exhibit direct spin-orbit coupling (SOC). [6, 7] Consequently, ISC processes would not be favored, as can easily be rationalized using Fermi’s Golden Rule. [8] Accordingly, other electronic states have to be introduced, when developing adequate TADF molecules. Such states can exhibit direct and/or vibronically induced couplings and thus, enhance ISC rates.

## 2. Non-conjugated bridges fixing donor and acceptor

Small overlap of the molecular orbitals of donor and acceptor, giving small  $\Delta E(S_1-T_1)$ , can be realized by increasing the spatial distance between both moieties. In Figure 1, a corresponding structure type is displayed together with an example molecule (compound 1). In Figure 1c, we reproduce the frontier orbitals as resulting from DFT calculations at the B3LYP/6-311G\*\* level of theory. It is clearly seen that the molecular orbitals, the natural transition orbitals (essentially representing HOMO and LUMO), show very small overlap allowing us to predict a small quantum-mechanical exchange interaction and a small energy gap between the  $^1,^3CT$  states. Presumably, the overlap is largely determined by a residual hyper-conjugation. Indeed, TD-DFT calculations carried out for the optimized geometry of the lowest  $^3CT$  state in vacuum gives, as a rough estimate, an energy gap of  $\Delta E(^1CT(S_1) - ^3CT(T_1)) \approx 50 \text{ cm}^{-1}$  (6 meV). Almost the same gap is found using two different functionals for the TD-DFT calculations (B3LYP and M06). For such a small energy gap, being a consequence of a the small HOMO-LUMO overlap, one also expects to find a weak oscillator strength  $f(S_1 \rightarrow S_0)$  or a weak allowedness for the  $S_1 \rightarrow S_0$  transition. [5] In fact, TD-DFT calculations allow us to estimate the oscillator strength to  $f(S_1 \rightarrow S_0) \approx 0.00145$ . We assume that this value describes at least the order of magnitude correctly and thus, can help us to understand important photophysical properties. Below it will be shown that this is justified.

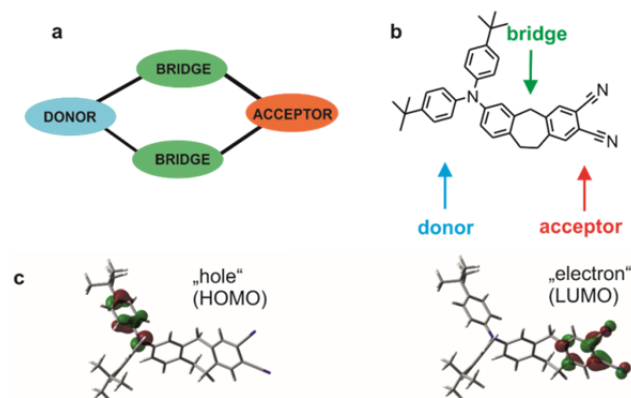


**Figure 1.** (a) Structure concept for a TADF material with donor and acceptor bound by two non-conjugated bridges. (b) Compound 1 as an example molecule. (c) Contour plots of natural transition orbitals for the  $S_0 \rightarrow ^3CT(T_1)$  excitation. “Hole” and “electron” correspond largely to HOMO and LUMO of the non-excited molecule, respectively.

Figure 2 reproduces emission properties of compound **1** measured at  $T = 300$  K in toluene. The emission color is white blue peaking at  $\lambda(\text{max}) = 476$  nm. (Figure 2a) The emission decay dynamics shows a two-component behavior. The short component is assigned to the prompt fluorescence with  $\tau(\text{prompt}) = 270$  ns, while the long one with  $\tau = 9$   $\mu\text{s}$  represents the TADF decay. (Figure 2b) Adapted to these decay times, time-resolved spectra were recorded for the ranges of the prompt fluorescence with no time delay ( $t = 0$  ns) and with a time-window of  $\Delta t = 80$  ns and for the delayed fluorescence with  $t = 5$   $\mu\text{s}$  and  $\Delta t = 30$   $\mu\text{s}$ , respectively. The two resulting time-resolved spectra show a complete overlap of prompt and delayed fluorescence as expected, since the same  $S_1 \rightarrow S_0$  transition is involved for both types of transitions. A similar behavior is also found for compound **1** doped in polystyrene (showing a 28 nm blue-shifted emission). Interestingly, for many other TADF compounds, the delayed fluorescence is red shifted with respect to the prompt fluorescence. This is ascribed to the inhomogeneous distribution of the organic TADF molecule in a rigid host matrix. Obviously, the design of our compound **1** (and of compound **2**, as shown below) is perfectly suited to suppress this unfavorable behavior.

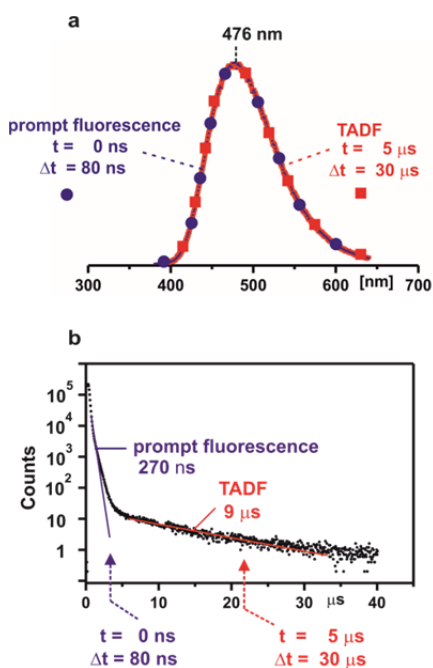


**Figure 2.** (a) Time-resolved emission spectra of compound **1** measured at  $T = 300$  K dissolved in toluene at  $c \approx 10^{-5}$  Mol/L,  $\lambda(\text{exc}) = 355$  nm, excitation pulse width 10 ns. (b) Emission decay plot of compound **1** measured under same conditions. The time-ranges for the time-resolved emission spectra as displayed in (a) are indicated,  $\lambda(\text{det}) = 470$  nm

For completeness, it is mentioned that the calculated oscillator strength of  $f(S_0 \rightarrow S_1) \approx 0.00145$  can be used to very roughly estimate the radiative rate of the corresponding transition according to: [9]

$$k^f(S_1 \rightarrow S_0) \approx \nu_{0-0}^2 f(S_0 \rightarrow S_1) \quad (1)$$

herein  $k^f(S_1 \rightarrow S_0)$  is the radiative rate of the  $S_1 \rightarrow S_0$  transition and  $\nu_{0-0}$  is its 0-0 transition energy measured in  $\text{cm}^{-1}$ . With  $\nu_{0-0} \approx 25\,000$   $\text{cm}^{-1}$  of compound **1** (Figure 2a), we obtain a radiative

fluorescence decay rate of  $\approx 1.1$   $\mu\text{s}$ . If we roughly assume that the contribution to the quantum yield of the prompt fluorescence amounts to about one half of the total quantum yield of  $\approx 30\%$ , we find a decay time of  $\approx 170$  ns. This is in rough agreement with the experimentally determined value of 270 ns.

The two low-lying states represent  $^{1,3}\text{CT}$  states split by  $\approx 50$   $\text{cm}^{-1}$  (6 meV) and show prompt and delayed fluorescence, respectively. In addition, at least one further triplet state lies energetically less than 1 eV higher as shown by TD-DFT calculations. Obviously, the existence of this state in energy proximity to the  $^{1,3}\text{CT}$  states has important implications. Such locally excited ( $^3\text{LE}$ ) states may provide different wavefunction character to the  $^1\text{CT}$  and  $^3\text{CT}$  states by quantum-mechanical couplings and thus, open the down- and up-ISC processes. However, the mixings of the  $^3\text{LE}$  state by configuration interaction (CI) with the  $^3\text{CT}$  state and by spin-orbit coupling (SOC) with the  $^1\text{CT}$  state are weak. Additionally, vibronic coupling can also alter the pure character of the  $^{1,3}\text{CT}$  states. [10, 11] In conclusion, already the discussed weak admixtures of different state character will provide some allowedness to the ISC processes and induce sufficient admixtures to allow for the TADF occurrence in the emission of compound **1**.

In the next section, we want to present a material that will exhibit distinctly more admixtures of other state character to the  $^{1,3}\text{CT}$  states. Moreover, this newly designed material features a drastically smaller singlet-triplet gap.

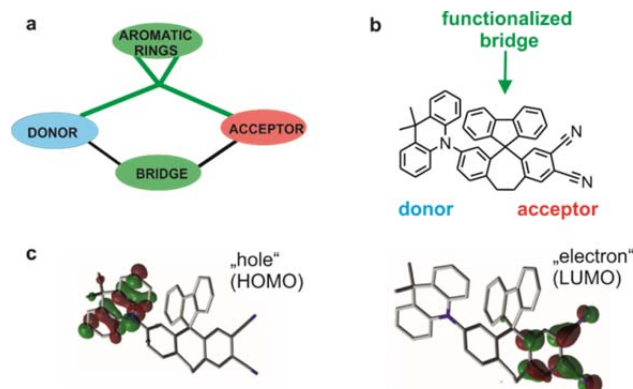
### 3. Functionalized donor-acceptor bridge: Reduction of hyper-conjugation and increase of the inter-system crossing rate

Figure 3 displays a new structure type and an example molecule (compound **2**). This compound is designed to follow two photophysical requirements: (i) The energy gap  $\Delta E(S_1-T_1)$  between singlet and triplet is pushed to a distinctly lower value than found for compound **1**. This is achieved by reducing the residual conjugation (hyper-conjugation) that still couples donor and acceptor electronically even via the non-conjugated bridge. (ii) The ISC rates between  $^1\text{CT}$  and  $^3\text{CT}$  become faster by mixing-in energetically close-lying triplet states. This leads to a faster equilibration and hence, a shorter overall decay time.

Interestingly, functionalization of the shorter one of the two bridges (Figure 3b) will meet the two requirements. The substitution largely “blocks” the hyper-conjugation between donor and acceptor. In addition, the selected biphenyl group provides several low-lying triplet states of  $^3\text{LE}$  character that will further modify the  $^{1,3}\text{CT}$  states by configuration interaction and spin-orbit coupling. Below we will demonstrate that this design strategy is highly successful.

DFT calculations carried out at the B3LYP/6-311 G\*\* level of theory for the optimized geometry of the lowest  $^3\text{CT}$  state (in vacuum) provide HOMO (hole) and LUMO (electron) contour plots. The distributions displayed in Figure 3c show that the corresponding overlap is very small. Indeed, TD-DFT calculations with two different functionals (M06 and B3LYP) give an energy separation of  $\Delta E(^1\text{CT}(S_1) - ^3\text{CT}(T_1)) \approx 10$   $\text{cm}^{-1}$  (1.2 meV) (for both theoretical estimates). Moreover, TD-DFT calculations show three additional triplet states that lie within less than 1 eV above the  $^{1,3}\text{CT}$  states. In particular, the state of nearest vicinity is calculated to be only about 0.2 eV apart. On the other hand, experimentally at least three localized states can

be identified lying in energy vicinity of 0.4 eV to the  $^1\text{CT}$  states. These represent  $^3\text{LE}$  states that involve the biphenyl substitution, designated as  $^3\text{LE}(\text{biphenyl})$ ,  $^3\text{LE}(\text{donor})$ , and  $^3\text{LE}(\text{acceptor})$ , according to the leading contributions. The relative positions of  $^1\text{CT}$  and the localized states are very sensitive to the polarity of the environment, as experimentally confirmed. Thus, at ambient temperature of compound **2** dissolved in toluene, the  $^3\text{LE}(\text{biphenyl})$  state is identified to lie only several 10 meV apart.



**Figure 3.** (a) Structure concept for a new material with donor and acceptor bound by two non-conjugated bridges containing a biphenyl substitution for reduction of hyper-conjugation and for providing additional couplings by configuration interaction and spin-orbit coupling. (b) Compound **2** as a concept example. (c) Contour plots of natural transition orbitals for the  $S_0 \rightarrow {}^3\text{CT}(T_1)$  excitation. "Hole" and "electron" correspond largely to HOMO and LUMO of the non-excited molecule, respectively.

Figure 4 reproduces the ambient-temperature cw photoluminescence spectrum of compound **2** dissolved in toluene. The spectrum is very broad as expected for a CT transition and the emission decay is strictly mono-exponential over more than three orders of magnitude decaying with 420 ns. No long-lived component that might be assignable as TADF is observed. Time-resolved spectra detected for any time range from several ns to about 3  $\mu\text{s}$  are identical and almost equal to the cw emission spectrum. With the emission quantum yield of  $\Phi_{\text{PL}}(\text{degassed}) = 65\%$ , a radiative rate of  $k^r = 1.5 \cdot 10^6 \text{ s}^{-1}$  is obtained. This rate is almost constant when cooling the compound. The emission band exhibits a strong red shift with increasing polarity, for example, with temperature decrease. [12] This is consistent with the CT character of the transition and excludes an assignment as localized transition.

Based on the results obtained, we have to conclude that a specific long-lived TADF is not occurring. This is not unexpected, since the two states  $^1\text{CT}$  and  $^3\text{CT}$  have almost the same energy. Referring to the thermal energy available at  $T = 300 \text{ K}$  of  $210 \text{ cm}^{-1}$  (26 meV), the small energy gap of  $10 \text{ cm}^{-1}$  (1.2 meV) is neglectable. Accordingly,  $^1\text{CT}$  and  $^3\text{CT}$  may be regarded as being almost iso-energetic. Below, we will argue that both states are in a fast thermal equilibrium. In this respect, "fast" is related to the observed decay time of 420 ns. For completeness, it is stressed that the involvement of the  $^3\text{CT}$  state in the emission process is further strongly supported by the efficient emission quenching observed under air saturation.

Oxygen induces with preference quenching of the triplet state population. As a consequence, it is concluded that the emission observed represents an averaged decay from both states. Obviously, this averaged decay time is significantly shorter than obtainable so far with compounds exhibiting time-delaying TADF processes.

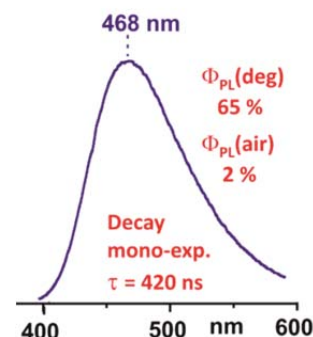


**Figure 4.** Time-integrated (cw) emission spectrum of compound **2** measured at  $T = 300 \text{ K}$  dissolved in toluene at  $c \approx 10^{-5} \text{ mol/L}$ .  $\lambda(\text{exc}) = 310 \text{ nm}$ . Time-resolved spectra detected for any time range from several ns to about 3  $\mu\text{s}$  are identical with the cw emission spectrum.

As mentioned before, three triplet states or more exactly 9 substates that result from different configurations can mix their  $^3\text{LE}$  character to the  $^1\text{CT}$  state via SOC and their triplet character to the  $^3\text{CT}$  substates via configuration interaction. The lowest  $^3\text{LE}(\text{biphenyl})$  state is of particular importance, since its energy separation from the  $^1\text{CT}$  states amounts only to a few  $10^2 \text{ cm}^{-1}$  (a few 10 meV), depending on temperature and polarity of the environment, as may be concluded from temperature-dependent emission measurements in the range from 300 K to 200 K and at  $T = 77 \text{ K}$ , respectively. For example, cooling from  $T = 300 \text{ K}$  to 200 K red-shifts the CT emission by  $\approx 10^3 \text{ cm}^{-1}$  (125 meV) due to an increase of polarity. Moreover, vibronic coupling, not discussed here further, opens additional coupling routes.

In conclusion, the ISC rate may strongly speed up by multiple couplings to other energy states that have different character than the  $^1\text{CT}$  and  $^3\text{CT}$  states. According to Fermi's Golden Rule [8], the vibrational Franck-Condon (FC) factors for the two states are also of high relevance for ISC. Since both states of CT character have almost the same geometry, no essential rearrangements are required for the ISC processes. With other words, large FC factors will favor fast ISC.

These assignments may be related to a theoretical discussion of ISC rates that has recently been carried out for a number of other compounds. [13] There, it was shown that at a very small energy gap and at a SOC coupling energy between singlet and triplet of only  $0.8 \text{ cm}^{-1}$  (0.1 meV) an ISC time of less than 10 ns may occur. A similar situation seems to be realized with compound **2** (but not with compound **1** that shows less coupling routes). For this specifically designed material **2**, we (i) minimized the energy gap between the lowest  $^1\text{CT}$  and  $^3\text{CT}$  states, (ii) maximized the FC factors, and (iii) optimized SOC. However, with our experimental equipment, we could not yet measure the ISC time of a few ns directly. On the other hand, longer decay times up to many  $\mu\text{s}$  would have been easily detectable (for example, see Figure 2). However, such long components are not observed for compound **2**. Therefore, we conclude that the ISC

process is fast and leads to a fast thermal equilibration between  $^1\text{CT}$  and  $^3\text{CT}$ .

#### 4. Concluding outlook: Towards fourth generation OLEDs

The new material concept, designed to exhibit (i) an almost “zero-gap” energy between the low-lying singlet and triplet states of charge transfer character and (ii) a significant number of coupling routes to other energy states. This leads to fast intersystem crossing and thus, fast equilibration between singlet and triplet. For these processes thermal activation at  $T = 300\text{ K}$  is not a key requirement. If the emitter is applied in an OLED, fast ISC will transfer or harvest all singlet and triplet excitons “directly” in the lowest singlet state ( $^1\text{CT}$ ) without the need of time-delaying TADF processes. Hence, this mechanism has been designated as *Direct Singlet Harvesting (DSH)* mechanism.[14] Its great advantage for OLED use lies in a significant reduction of the overall emission decay time. This mechanism leads us to beyond TADF and towards a fourth generation OLED mechanism that opens the way for reducing stability problems and roll-off effects. We are convinced that this new material concept will successfully stimulate substantial progress in organic electronics.

#### 5. References

- [1] C. A. Parker, C. G. Hatchard, *Trans. Faraday Soc.* **1961**, 57, 1894.
- [2] H. Yersin, U. Monkowius, Komplexe mit kleinen Singulett-Triplett-Energie-Abständen zur Verwendung in opto-elektronischen Bauteilen (Singulett-Harvesting-Effekt). Internal patent filing, University of Regensburg 2006. German Patent DE 10 2008 033563, **2008**.
- [3] H. Yersin, ed., *Highly efficient OLEDs – Materials based on Thermally Activated Delayed Fluorescence*, Wiley-VCH, Weinheim, Germany **2018**, DOI: 10.1002/9783527691722
- [4] H. Uoyama, K. Goushi, K. Shizu, H. Nomura, C. Adachi, *Nature* **2012**, 492, 234-238.
- [5] R. Czerwieńiec, M. J. Leitl, H. H. H. Homeier, H. Yersin, *Coord. Chem. Rev.* **2016**, 325, 2 – 28.
- [6] M. A. El-Sayed, *J. Chem. Phys.* **1963**, 38, 2834-2838.
- [7] A. F. Rausch, H. H. H. Homeier, H. Yersin, *Top. Organomet. Chem.* **2010**, 29, 193 – 235
- [8] J. A. Barltrop, J. D. Coyle, *Excited states in organic chemistry*, Wiley London **1975**, p. 88.
- [9] N. J. Turro, *Modern Molecular Chemistry*, Benjamin/Cummings, Menlo Park, California **1978**.
- [10] C. M. Marian, J. Föllner, M. Kleinschmidt, M. Etinski, *Intersystem crossing processes in TADF emitters. In: Highly Efficient OLEDs. Materials Based on TADF*, ed. H. Yersin, Wiley-VCH, Weinheim Germany **2018**, DOI: 10.1002/9783527691722
- [11] T. J. Penfold, J. Gibson, *The role of vibronic coupling for intersystem crossing and reverse intersystem crossing rates in TADF molecules. In: Highly Efficient OLEDs. Materials Based on TADF*, ed. H. Yersin, Wiley-VCH, Weinheim Germany **2018**, DOI: 10.1002/9783527691722
- [12] F. I. Mopsik, *J. Chem. Phys.* **1969**, 50, 2559 – 2569
- [13] P. K. Samanta, D. Kim, V. Coropceanu, J.-L. Brédas, *J. Am. Chem. Soc.* **2017**, 139, 4042 – 4051
- [14] (a) H. Yersin, L. Mataranga-Popa, R. Czerwieńiec, *Design of organic TADF molecules. The role of  $\Delta E(S_1-T_1)$ : From fluorescence to TADF and beyond – towards the fourth generation OLED mechanism*, 22nd International Krutyn Summer School, Krutyn, **2017** <http://www.excilight.com/node/203>.  
(b) H. Yersin, L. Mataranga-Popa, R. Czerwieńiec, Organische Moleküle für Direktes Singulett-Harvesting mit kurzer Emissionsabklingzeit zur Verwendung in optoelektronischen Vorrichtungen. European patent EP 17170682.3, **2017** and German patent DE 10 2017 101432.2, **2017**.